Characterization of Nigerian bloomery iron smelting slags

J A Whiteman and E E Okafor

ABSTRACT: *Fifty-one bloomery iron smelting slags from four sites in the Nsukka Division of Nigeria have been characterized. Radiocarbon dating has shown that smelting in this area took place over about two millennia. The chemical compositions of typical phase mixtures and individual phases were determined using EDS analysis in an SEM, and phase proportions were obtained from the SEM back-scattered electron images and by point counting of optical microscopy images. All the slags were essentially contained within the Al_2O_3–SiO_2–FeO ternary system, with the major phases being fayalite, hercynite and glass, with wüstite in some of the earlier slags. The liquidus temperature of the slags could be inferred from the ternary diagram. The earliest slags, which had high liquidus temperatures, could have been made directly from ore currently found on site; these slags were tapped into slag pits. Later slags had lower liquidus temperatures and in general could not have been made from current ores; they were raked out of the furnace as agglomerates. Mass balance calculations showed that the later slags were associated with a higher output of iron per unit of charged ore. The change in liquidus temperature is associated with a change in smelting technology from forced draught to natural draught furnaces, and a change in slag removal method. It is concluded that ore sizing was carried out at all the sites, and that sand or ore fines were added to the burden at the later sites.*

Introduction

There is a considerable literature on bloomery ironmaking in Nigeria, which has been examined by Okafor (1992). The essential findings from the historical and oral tradition are that bloomery ironmaking in Nsukka is very ancient, that the technology spread from Nsukka to other Nigerian ironmaking communities, and that it continued until recent times. However, there was no direct evidence as to the age of the sites in the region. The other important issue in Nigerian bloomery ironmaking is the development of the natural-draught tall furnace (van der Meerwe 1980).

Analysis of bloomery ironmaking slags and residues is uncommon. The potential for characterization of such material was demonstrated by Morton and Wingrove (1969, 1972), who analysed slags from a number of Roman and medieval British bloomery sites and based their compositions on the anorthite-SiO_2-FeO system. More recently Photos-Jones *et al* (1998) produced detailed analyses of Scottish bloomery residues, Høst-Madson and Buchwald (1999) some slag data from Snorup in Denmark, and Benevuti *et al* (2000) compositions of slags and other residues from Populonia in Italy. Challis (2002) reported some analyses of medieval iron slags from Stanley Grange in England, and related them to the types of shaft furnace employed. Apart from Photos-Jones *et al* (ibid), who plotted their results on a pseudo-ternary phase diagram, none of these later workers attempted to analyse their European slag compositional data in any detail.

West African slags and residues have been analysed by Tylecote (1975) and Goucher (1981). The most comprehensive work on African ironmaking was done on Ethiopian residues by Todd and Charles (1978) and Todd (1979, 1984), who developed the technique of inclusion analysis in iron artefacts to provenance material. The techniques used in those investigations are well described by Bachmann (1982). Recent work by Inge and Rehren (2003) on bloomery slags in Modakeke, south-west Nigeria, has shown that there ilmenitic black sand and lateritic ores were mixed together in bloomery iron making and resulted in slags with a high titania content.

Analysis of bloomery slags has been supplemented by experimental work simulating the operation of bloomery furnaces. For example Tylecote *et al* (1971)

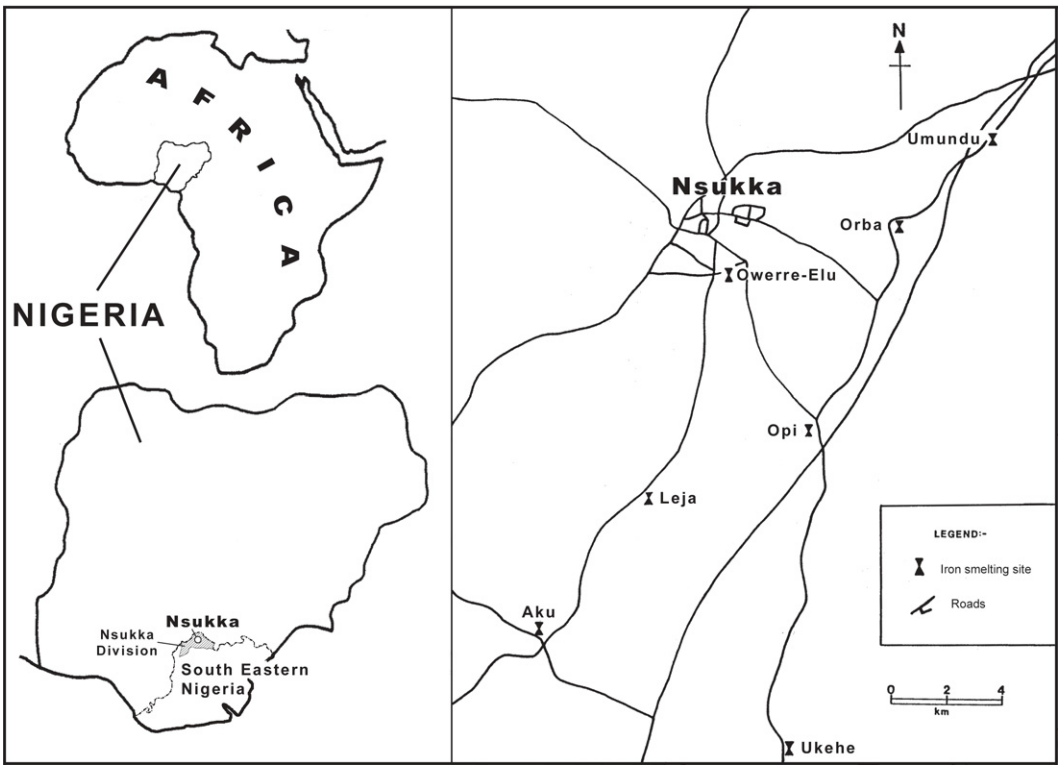

Figure 1: Locations of iron bloomery sites in the Nsukka area of Nigeria. The four most northerly sites were the subject of the present investigation.

clearly identified the factors that control both the possibility and efficiency of bloomery furnace operation. These include a need for sizing ore, the importance of bed-depth in providing indirect reduction, and the influence of fuel-to-ore ratio in controlling the chemical composition of the iron and slag fluidity. They also analysed some of the slags produced in their experimental work. This work has direct relevance to the investigation reported here.

No systematic work has been carried out on slags from the Nsukka division of Nigeria, although the samples for such a study had been collected by Okafor (1992), together with ethnographical and oral information from each of the sites. The position of the sites is shown in the maps in Figure 1. Table 1 summarizes the important features of the four sites from which the slag samples were obtained. The slag residues from the four sites were radiocarbon dated through charcoal embedded in the slags and typically three dates were obtained for each site. The two from Owerre-Elu were made from fused wood and straw associated with the clay used for the tuyeres, and embedded in the slag. The carbon dating was carried out at the Oxford Accelerator Mass Spectroscopy Laboratory using the calibration curve of Stuiver and Pearson (1986) and the calibration programme of van der Plicht and Mook (1989). The possibility of old wood having been used is discussed by Okafor (1992), who concludes that this was unlikely.

The oldest site is Opi, in which smelting was carried out in the later first millennium BC. Owerre-Elu is a site of intermediate age with dates from the first millennium AD and into the second millennium AD. The two sites of Orba and Umundu are the most recent with smelting during the last four centuries. It seems likely that the sites were used in succession by smelters who moved to a new one when the local resources, probably of timber, were exhausted, and that iron making has taken place in the Nsukka area for well over 2000 years, possibly continuously and certainly until very recent times. Ores obtained from deposits near each smelting site were either hematite or goethite, with both being found at Umundu.

Two types of shaft furnace were employed for smelting: forced draught at the older sites and natural draught at the more recent sites. Successive slags were tapped into pits at Opi and at Owerre-Elu, but in the later operations the slag was raked out of the furnace as an agglomerate. Charcoal obtained from hardwood was used at three of the furnace sites, but hardwood was used directly in the furnaces at Orba. It is also recorded that sand was added to the Orba furnace (Okafor 1992).

Sampling

Because of the very large amounts of slag at these sites, it was necessary to sample efficiently. Each site was surveyed to determine the dimensions and variations

within it, then zoned into residue-cluster areas. The number of samples collected from each area depended on the quantity and variety of residues in each zone, and are listed in Table 1. All were well-formed slags with smooth surfaces. Samples for analysis were small lumps, typically less than 50mm in maximum dimension, broken from the tapped or raked slag masses. Ore samples were collected from all of the sites with at least two samples being taken from each.

Experimental Method

Pieces of slag were sliced into thin sections about 15 x 15 x 3mm using a diamond saw. These sections were then ground on silicon carbide papers, diamond-polished, mounted on aluminium stubs and coated with a thin surface film of carbon to prevent charging in the scanning electron microscope (SEM).

The SEM was a Camscan 2 with a Link energy-dispersive X-ray spectroscopy (EDS) system and KE back-scattered electron (BSE) detector, operated at 20kV to give an effective X-ray penetration depth for the phases with lowest atomic number of approximately 3μm. Three separate areas, about 0.5 x 0.35mm on each sample, were examined using the BSE image. Each area was photographed and the image analysed using Link Digipad software to measure the volumetric phase proportions. The area was then scanned to provide a 'bulk' EDS analysis (wt%) using the ZAF4 quantitative analysis programme. The standards used in the quantitative analysis of Si, Al and Fe were quartz, alumina, and a synthetic FeO. Other elements were analysed using non-standards reference spectra. Stoichiometry was assumed for each of the oxides and the analysis reported on the basis of the oxides totalling 100%. Three area analyses were obtained from each specimen and individual phase spot analysis was performed in each area analysed.

To ensure that the phase proportions and the overall composition were sensibly related to each other a computer program was written, which used the analysed composition of each major oxide phase, an assumed phase density, and the measured volumetric phase proportion to calculate the overall chemical composition as percentage by weight. This was then compared with the analysis obtained from the area scans. If there was significant difference between them, the specimen was re-analysed in the SEM. In the event only three of the 51 samples were considered to be sufficiently different to warrant further analysis. In each anomalous case there was some interference of one minor phase with an adjoining major phase due to the small size of the minor phase particles. The phase proportions obtained by the Digipad image-analysis programme were checked by point-counting the proportions of the constituent phases in the photomicrographs obtained from each specimen.

Ore samples were mounted and polished in a similar way to the slag samples and examined by the same process in the SEM. Ore samples and a selection of slag samples were analysed by X-ray diffraction to determine the crystal structures of the various phases present.

Results

The slags found at any site had a range of composition and, although there is considerable

Table 1: Characteristics of iron bloomery sites in Nsukka

Site characteristics	Opi	Owerre-Elu	Orba	Umundu
Age range*	2305±90 BP 2170±98 BP 2080±90 BP	1060±60 BP 570±60 BP	300±90 BP 295±85 BP 215±100 BP	200±80 BP 205±80 BP 130±80 BP
Area covered	> 30,000m^2	55,000m^2	4,500m^2	8,500m^2
Type of ore	hematite	hematite	goethite, sand added	goethite and hematite
Fuel used	charcoal	charcoal	hardwood	charcoal
Furnace type	forced draught shaft	forced draught shaft	natural draught shaft internal wooden frame	natural draught shaft
Slag	cylindrical blocks tapped into pits	flattish tapped slag with ropey surface	raked aggregates	raked aggregates
No. of slag samples analysed	15	12	12	12

Note: * = individual ^{14}C dates from charcoal embedded in slag, measured in 1991

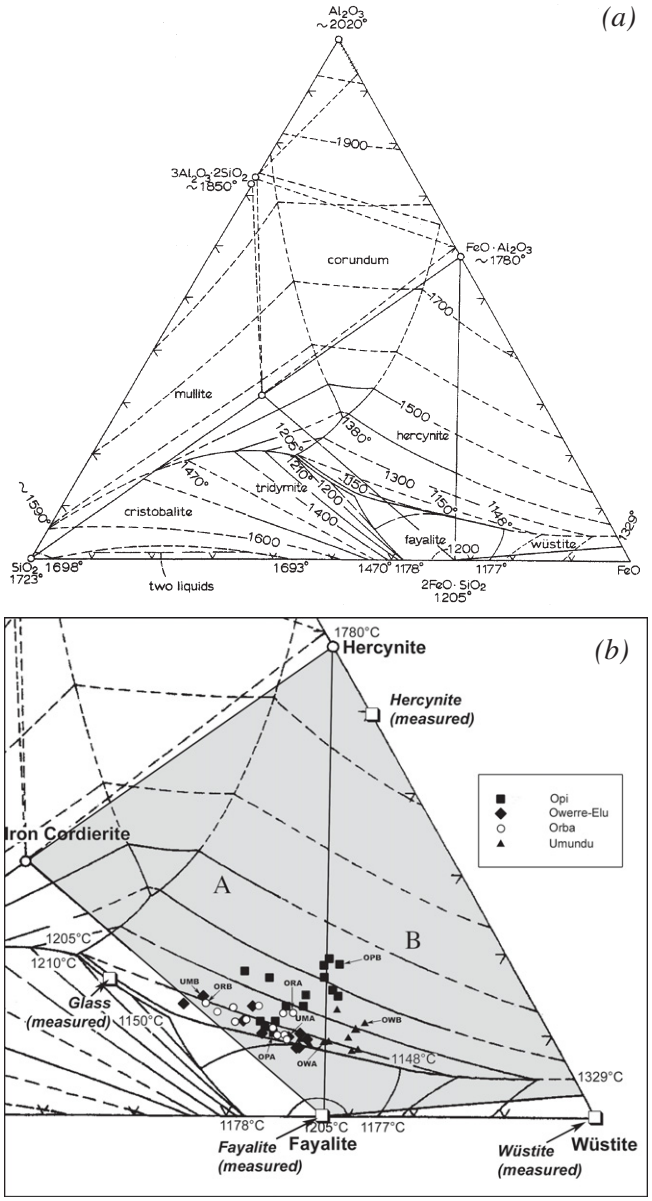

Figure 2: (a) FeO-Al_2O_3-SiO_2 ternary phase diagram (Lewin et al 1964, 869), (b) section of diagram showing compositions of all analysed slags.

overlap in composition of slag from different sites, there are compositions particular to each site. Figure 2a shows the Al_2O_3-SiO_2-FeO ternary phase diagram, and 2b the compositions of all the slags that were analysed on part of that same diagram, presented as wt%. In order to plot these points on a ternary diagram, the quantities of the three major oxide components were normalized to 100%.

Table 2 gives more complete analyses of two slags with widely different microstructures from each site. For each site, slag 'A' is typical of the compositions that overlap and slag 'B' is typical of the compositions particular to the site. All the 'A' compositions are fairly close to the mean analysis of all the slags which is 58.8% FeO, 11.3% Al_2O_3, 26.1% SiO_2 , and similar to that of the two slags from Nuns Well reported by Morton and Wingrove (1972). In all cases the major oxides wüstite, alumina and silica totalled 95% or more, but small amounts of other oxides were present, notably TiO_2 at an average value of 1.6% was present in all the slags. The component with greatest variability was alumina. The mean Al_2O_3/SiO_2 ratio for all the slags is 0.435.

The ores found at the four major sites were analysed in the SEM and their chemical compositions are shown in Table 3. A micrograph of a typical ore is shown in Figure 3. All the ores contained three constituents, which can be seen in the BSE image, with some variation in their proportions. The lightest phase is Fe_2O_3, the intermediate grey phase a clay mineral and the darkest phase silica. Although some qualitative analysis was attempted, the particles were too small for consistent quantitative analysis. The mean Al_2O_3/SiO_2 ratio for the ores (excluding OP02, which has too low an iron-to-silica ratio to make a slag), is 0.747. The ores are higher in alumina than any reported from Carboniferous Period by Morton and Wingrove (1974), but not unlike those from Ethiopia examined by Todd (1979, 1984).

The compositions of the individual phases in each slag were also measured by spot analysis in the SEM. The averaged results over all the slags analysed showed that fayalite ($2FeO.SiO_2$) contained 69% FeO and 31% SiO_2, and wüstite (FeO) contained virtually 100% FeO, both

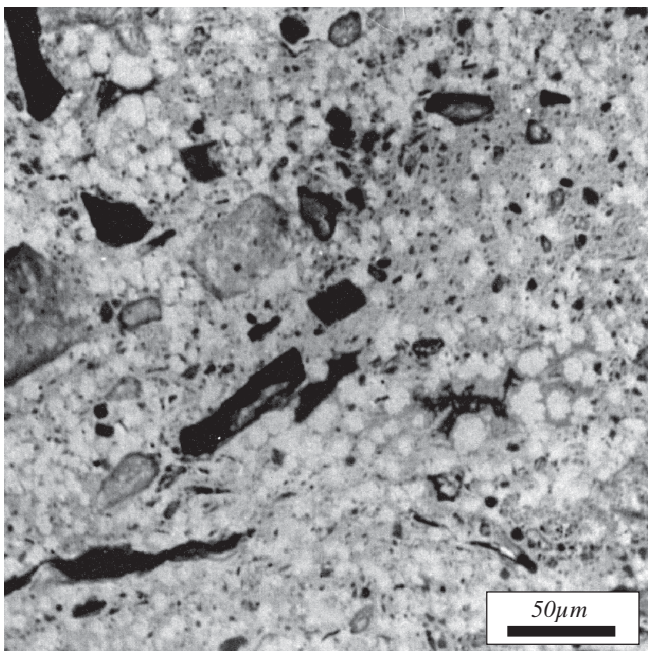

Figure 3: Microstructure of typical ore (OR01) BSE image.

Table 2: Normalized compositions and phase proportions of selected slags

	Opi				Owerre-Elu				Orba				Umundu			
Slag*	OPA		OPB		OWA		OWB		ORA		ORB		UMA		UMB	
	Composition (wt% oxide)															
	Mean	SD	Mean	SD	Mean	SD	Mean	SD	Mean	SD	Mean	SD	Mean	SD	Mean	SD
FeO	57.00	0.30	61.10	1.07	64.20	1.13	66.70	1.58	60.10	1.27	49.80	0.33	60.20	1.23	49.40	0.37
Al_2O_3	9.46	0.19	17.66	2.26	8.46	0.53	10.40	1.88	12.00	1.18	13.20	0.31	9.26	0.45	14.00	0.09
MgO	0.27	0.33	0.39	0.29	0.08	0.11	0.30	0.25	0.12	0.11	0.34	0.27	nd	nd	0.21	0.29
SiO_2	27.90	0.17	17.80	1.24	24.30	0.33	19.00	0.94	26.00	0.82	33.50	0.48	27.40	0.44	33.60	0.34
TiO_2	1.00	0.07	1.18	0.16	1.40	0.12	1.60	0.07	1.18	0.20	1.70	0.12	1.38	0.08	1.43	0.12
MnO	0.09	0.07	0.12	0.06	0.40	0.11	0.57	0.12	0.03	0.04	0.13	0.13	nd	nd	0.17	0.07
P_2O_5	1.73	0.09	0.83	0.18	0.51	0.07	0.73	0.13	0.42	0.02	0.86	0.28	0.63	0.14	0.34	0.04
CaO	1.36	0.17	0.35	0.13	0.31	0.03	0.53	0.07	0.11	0.07	0.14	0.03	0.61	0.02	0.37	0.09
S	0.09	0.07	0.06	0.08	0.03	0.04	nd	nd	0.03	0.04	0.13	0.08	0.09	0.07	0.09	0.07
V_2O_5	0.02	0.02	0.29	0.07	0.08	0.07	0.06	0.06	nd	nd	0.03	0.04	0.07	0.10	0.15	0.12
K_2O	1.08	0.09	0.18	0.01	0.25	0.07	0.07	0.03	nd	nd	0.20	0.06	0.42	0.07	0.26	0.05
Total	100	-	100	-	100	-	100	-	100	-	100	-	100	-	100	-
	Relative volume of phases (%)															
Fayalite	69	-	55	-	71	-	81	-	73	-	45	-	58	-	46	-
Hercynite	13	-	33	-	21	-	15	-	18	-	12	-	13	-	10	-
Glass	-	-	-	-	4	-	4	-	9	-	42	-	29	-	44	-
Wüstite	7	-	8	-	4	-	-	-	-	-	-	-	-	-	-	-
Leucite	11	-	3	-	-	-	-	-	-	-	-	-	-	-	-	-

Notes: *These are selected examples of slags from each site. Those slags with suffix 'A' are of similar to those from the other sites; those with suffix 'B' are characteristic of the particular site. Each composition value is calculated from three area analyses; iron is assumed to be FeO. nd = not detected.

phases carrying very small amounts of other elements. However the hercynite ($FeO.Al_2O_3$) with 51% FeO and 49% Al_2O_3 was always very iron-rich compared with the stoichiometric ratio. These measured average phase compositions are shown superposed on the phase diagram of Figure 2b. Keissling and Lange (1964) have

Table 3: Compositions of the ores

	Opi		Owerre-Elu			Orba		Umundu	
Ores	OP01	OP02	OW01	OW02	OW03	OR01	OR02	UM01	UM02
	Composition (wt% oxide)								
Fe_2O_3	68.43	57.03	70.93	70.24	69.49	68.54	68.93	72.4	61.29
Al_2O_3	9.44	6.59	12.03	10.86	10.71	12.77	12.75	11.73	15.77
MgO	0.08	0.18	0.09	0.03	0.04	0.00	0.33	0.19	0.20
SiO_2	19.22	32.31	16.02	15.15	15.54	16.16	15.33	13.34	19.59
TiO_2	2.49	3.19	0.53	3.18	3.90	1.73	2.15	1.99	2.84
MnO	0.00	0.11	0.01	0.01	0.00	0.02	0.04	0.00	0.00
P_2O_5	0.20	0.36	0.11	0.34	0.06	0.56	0.20	0.23	0.06
CaO	0.00	0.02	0.09	0.01	0.07	0.09	0.02	0.05	0.13
S	0.03	0.04	0.07	0.08	0.03	0.05	0.06	0.02	0.02
V_2O_5	0.10	0.11	0.09	0.07	0.065	0.06	0.20	0.05	0.05
K_2O	0.02	0.05	0.02	0.02	0.037	0.02	0.00	0.06	0.05
Total Fe	51.40	42.30	53.34	52.86	52.25	51.49	51.81	54.62	45.69

Notes: Each value is calculated from three analyses. Iron is calculated as Fe_2O_3.

investigated the hercynite in synthetic slags and reported a wide range of compositions. The other phase with a very variable composition was the glass, defined as such by the absence of characteristic X-ray diffraction spectra. The glass often contained high proportions of oxides that were only minor constituents in the slag, but the average composition excluding these was 38% FeO, 17% Al_2O_3 and 45% SiO_2.

The relative proportions of the different phases were measured on three areas of each slag sample, and the mean values for the selected slags are shown in Table 2Again there is considerable variation in phase proportions in different specimens from all sites and these differences can be seen in the micrographs of Figures 4 to 7, which show examples of microstructures from each site.

Figure 2 is an equilibrium phase diagram, and as such is useful only as a guide to the actual solidification process in a rapidly-cooled, viscous slag with possibly substantial local variations in chemical composition. However, the essential features of Figure 2 in the area of interest are a steeply sloping liquidus surface running from the hercynite point to an eutectic trough formed by a gently-sloping liquidus surface from the fayalite point. This trough lies near and at a shallow angle to the SiO_2-FeO edge of the diagram. It slopes downwards to the left of the fayalite-hercynite line to a ternary point at 1150°C, and downwards to the right of the same line to a ternary point at 1148°C, the latter formed by the junctions of fayalite-wüstite and wüstite-hercynite troughs.

Figure 2 also shows that at low temperatures all the slags should lie within one of two three-phase fields: iron cordierite-fayalite-hercynite (labelled A in Figure 2b), and wüstite-fayalite-hercynite (B in Figure 2b). The two-phase field fayalite-hercynite which separates these appears to be extremely narrow, as the two end phases have negligible compositional range.

The solidification processes predicted from these features are as follows:-

Slags with compositions to the left of the fayalite-hercynite line, on the alumina-rich side of the eutectic trough, commence solidification by forming primary hercynite which continues until alumina depletion moves the liquid composition onto the eutectic trough. However, at this point the remaining liquid is already lower in iron than the fayalite-hercynite eutectic which then starts to form, so that as eutectic solidification proceeds, the liquid is progressively depleted in iron. The liquid composition thus moves along the eutectic trough to the fayalite-hercynite-tridymite ternary point where solidification is completed. Subsequent four-phase reactions in the solid state result in the removal of tridymite and formation of an iron cordierite: $2FeO.2Al_2O_3.5SiO_2$, so that at room temperature the slags should lie within the iron cordierite-fayalite-hercynite triangle *A* in Figure 2b.

Slags with compositions on the alumina side of the trough, to the right of the fayalite-hercynite line, initially follow the same solidification sequence until the eutectic trough is reached. But the liquid is then richer in iron than the fayalite-hercynite eutectic, and as solidification proceeds, its composition moves towards the fayalite-wüstite-hercynite point where solidification is completed. The resultant phases should lie within the hercynite-wüstite-fayalite three phase field at low temperatures, shown as triangle B in Figure 2b.

A few of the slags have compositions just on the fayalite side of the eutectic trough, on both sides of the fayalite-hercynite line. These would be predicted to solidify in the same way as the others, except that a very little primary fayalite, instead of hercynite, would initiate the solidification process.

When these predictions are compared with the actual metallographic structures of the slags, shown in Figures 4–7, a broad agreement is found, but there were significant modifications brought about by non-equilibrium cooling and additional elements.

The phases fayalite and hercynite were always found in slags whose composition lies within the triangle *A* of Figure 2b, but the third phase was a glass rather than iron cordierite, with an average composition beyond the tridymite-fayalite-hercynite eutectic point in the FeO-Al_2O_3-SiO_2 phase diagram (see Fig 2). In the *B* triangle of Figure 2b the three expected phases were always found, but sometimes there was also a small amount of glass. In a few of the slags from the Opi site a further phase, leucite ($K_2O.Al_2O_3.4SiO_2$), was found.

Figures 4–7 are BSE micrographs that demonstrate this finding. The phases have distinctly different grey levels in these images. The brightest phase is wüstite, which appears white in the micrographs and has a dendritic morphology. The light-grey phase that makes up most of the microstructure is fayalite, in the form of plates or needles, and is formed eutectically. Hercynite is somewhat darker grey and is formed as a primary and/or eutectic phase with the angular shape characteristic of a spinel. Glass and leucite are very dark. The two

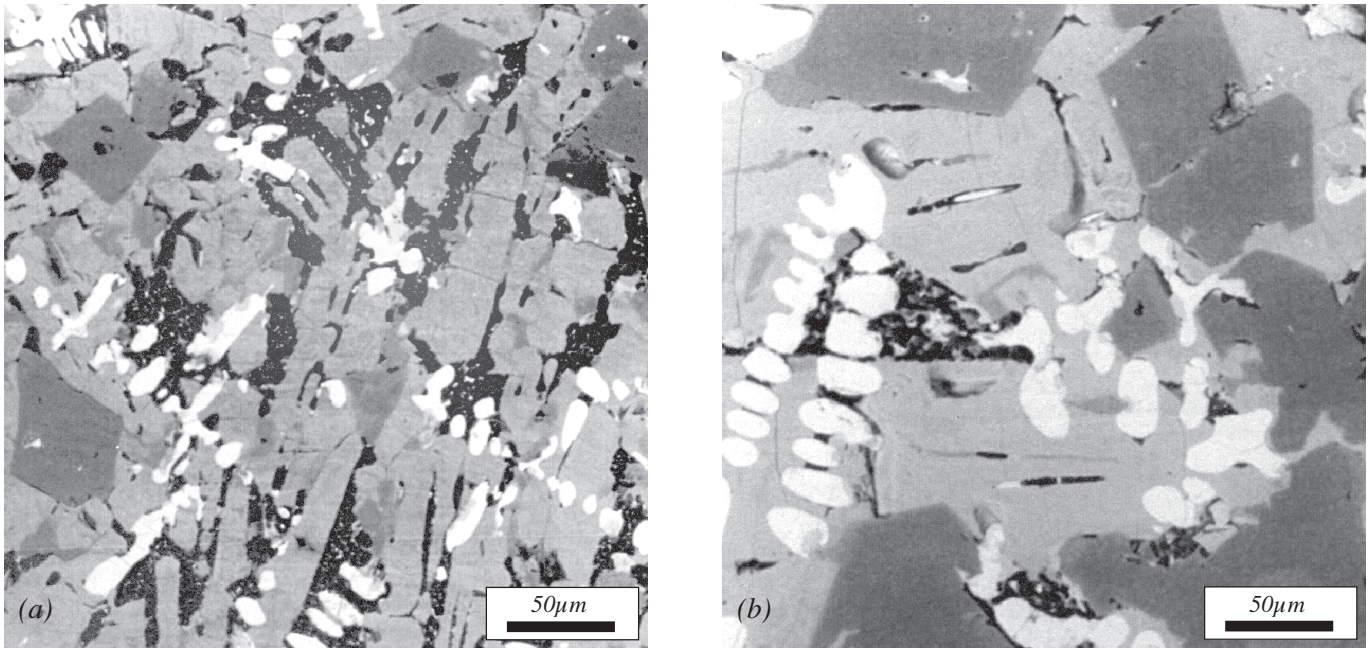

Figure 4: Microstructures of Opi slags, BSE images: (a) OPA, (b) OPB

basic types of microstructure are similar to those found in the Group A and Group C slags reported by Morton and Wingrove (1972).

Figure 4 shows the microstructures of the two slags from Opi whose analyses are listed in Table 2. Slag OPA (Fig 4a) lies in constitutive triangle *A* close to the eutectic valley. On cooling, primary hercynite was formed as dark-grey angular particles, followed by fayalite-hercynite eutectic. As predicted, the eutectic is predominately fayalite, and so appears as a mass of grey laths with very minor darker hercynite. Solidification was not completed and the remaining liquid exists as a glass containing some leucite. Wüstite would not be expected in this specimen, but exists in considerable quantities, confirming a substantial departure from the equilibrium diagram. Sample OPB (Fig 4b) is in the B constitutive triangle and also formed angular primary

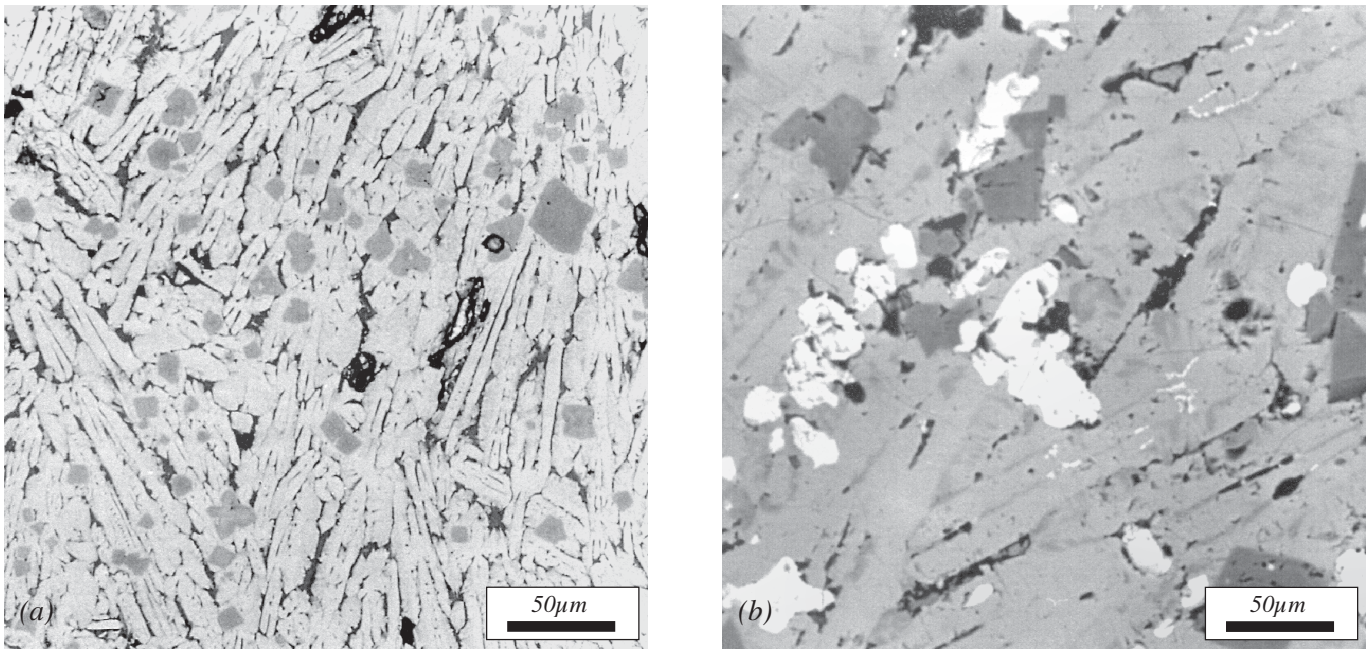

Figure 5: Microstructures of Owerre-Elu slags, BSE images: (a) OWA, (b) OWB

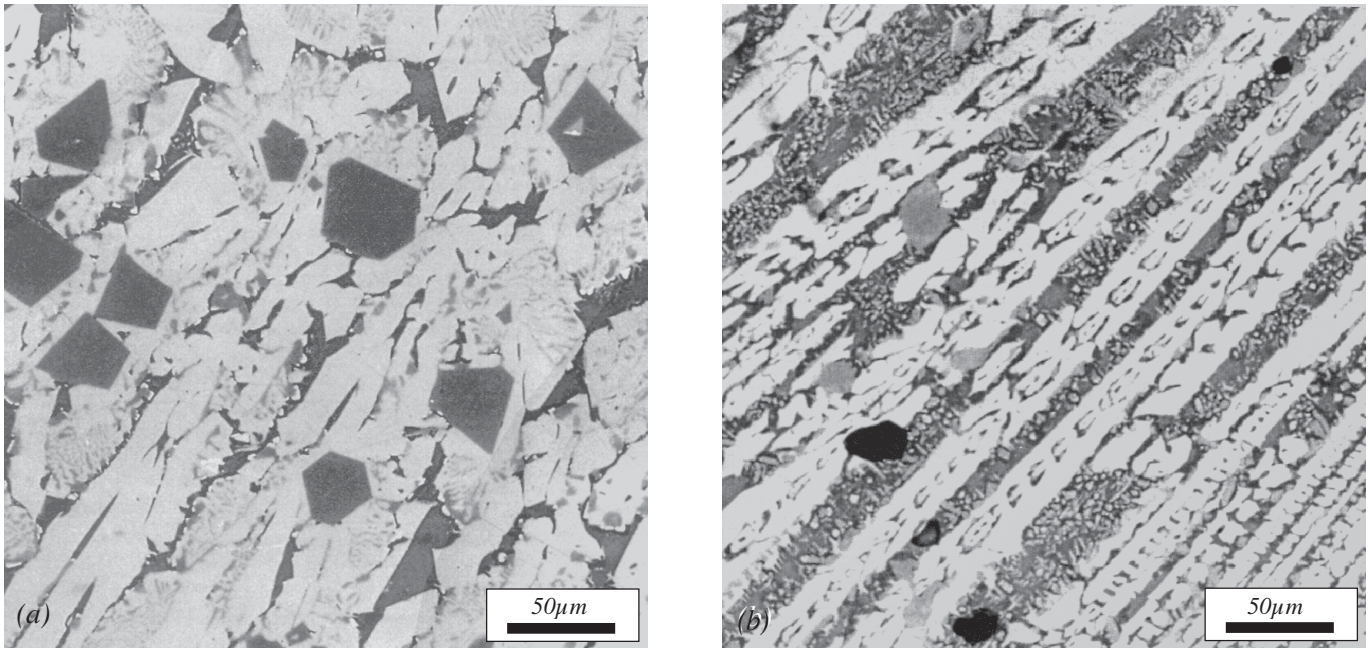

Figure 6: Microstructures of Orba slags, BSE images: (a) ORA, (b) ORB

hercynite and then the fayalite-hercynite eutectic. However, as predicted by Figure 2, this had moved the remaining liquid towards the ternary eutectic at 1148°C so that wüstite had formed along with hercynite and fayalite. The primary hercynite is clearly seen and the fayalite is the dominant phase in the eutectic. The lath size of the fayalite is larger than in OPA. There is a small amount of dark leucite in OPB.

None of the Opi slags, nor indeed any of the slags with the average compositions plotted on the ternary diagram, could produce primary wüstite, yet all the wüstite was dendritic in form. However the dendritic morphology of the wüstite does not necessarily imply a primary phase: such apparently 'primary' forms are not uncommon in many metallic eutectics (*eg* zinc aluminium alloys subject to rapid cooling, (Durman and Murphy 1994)), where undercooling allows the unrestricted formation of whichever eutectic phase is able to nucleate first from the supercooled liquid, and the same effect may be expected in oxide systems.

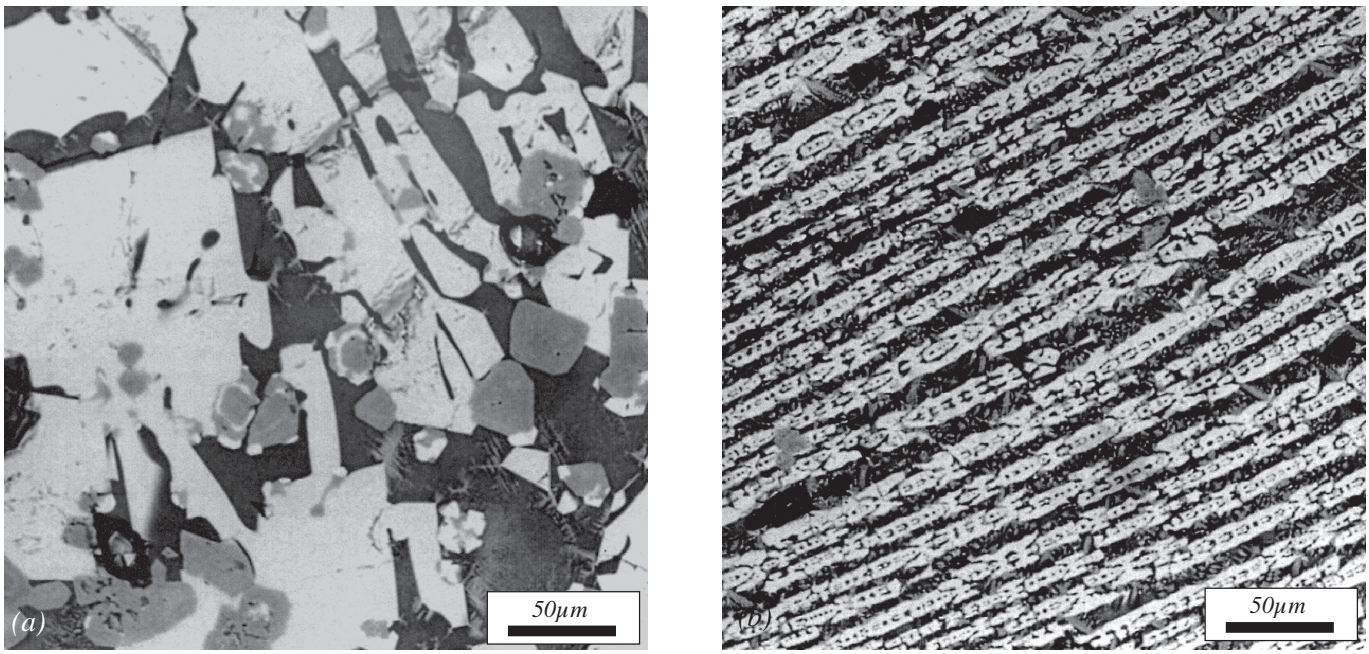

Figure 7: Microstructures of Umundu slags, BSE images: (a) UMA, (b) UMB

Figure 5 shows the microstructures in the two slags from Owerre-Elu. The microstructures of this slag are in good agreement with the phase diagram. OWA (Fig 5a) is just inside triangle A but very close to the boundary line between the two triangles. On cooling it had formed a very small amount of primary hercynite, which appears as a large angular particle in Figure 5a, followed by the fayalite-hercynite eutectic. There should be a very small amount of iron cordierite, but instead a larger than expected amount of glass was retained in the microstructure. Slag OWB (Fig 5b) is in the B constitutive triangle and had formed larger amounts of primary hercynite, followed by the fayalite-hercynite eutectic. At the ternary eutectic point wüstite had formed as expected, but some glass was also retained in this microstructure. The lath size of the fayalite, which makes up the majority of the slag, is larger in OWB than OWA.

Table 4: Mass balance 1 for the 'B' slags of Table 2

Oxide	BALANCE 1					
	Ore (kg)	Sand (kg)	Iron in (kg)	Iron out (kg)	Slag (kg)	Slag (wt%)
OPB						
Fe_2O_3	68.4	0.0	47.9	22.5	24.2	61.1
Al_2O_3	9.4	0.0	0.0	-	7.0	17.7
SiO_2	19.2	-12.1	0.0	-	7.1	17.8
Total wt	97.1	0.0	0.0	-	38.3	96.6
OWB						
Fe_2O_3	70.2	0.0	49.2	-6.7	71.8	66.7
Al_2O_3	11.2	0.0	0.0	-	11.2	10.4
SiO_2	15.6	4.9	0.0	-	20.5	19.0
Total wt	97.0	0.0	0.0	-	103.5	96.1
ORB						
Fe_2O_3	68.5	0.0	47.9	10.5	48.1	49.8
Al_2O_3	12.8	0.0	0.0	-	12.8	13.2
SiO_2	15.7	16.7	0.0	-	32.4	33.5
Total wt	97.0	0.0	0.0	-	93.3	96.5
UMB						
Fe_2O_3	66.8	0.0	46.7	9.0	48.5	49.4
Al_2O_3	13.8	0.0	0.0	-	13.8	14.0
SiO_2	16.5	16.5	0.0	-	33.0	33.6
Total wt	97.0	0.0	0.0	-	95.3	97.0
Mean ore					Mean slag	
Fe_2O_3	68.8	0.0	48.2	-0.4	62.4	58.8
Al_2O_3	12.0	0.0	0.0	-	12.0	11.3
SiO_2	16.3	11.4	0.0	-	27.7	26.1
Total wt	97.1	0.0	0.0	-	104.1	96.3

Note: For assumptions see text.

The two slags from Orba are shown in Figure 6; both lie in triangle A. Slag ORA (Fig 6a) is closer to the boundary between the two constitutive triangles and had produced primary hercynite on cooling followed by the fayalite-hercynite eutectic. Some glass is retained in the structure. Figure 6b shows that the solidification sequence in ORB was similar, with less primary hercynite formed. The higher silica content of this slag resulted in less fayalite-hercynite eutectic and more glass; the fayalite lath structure is also finer in this specimen.

The compositions of the two Umundu slags shown in Figure 7 are within the A constitutive triangle. UMB with its greater silica content is very close to the silica-rich boundary of the triangle, while the composition of UMA is close to that of ORA but nearer to the eutectic line. The UMA slag (Fig 7a), has some primary hercynite and much fayalite-hercynite eutectic. There is a considerable amount of glass and the fayalite lath size is large. In contrast the UMB slag (Fig 7b) has very little primary hercynite and is mainly fayalite-hercynite eutectic and glass. The lath structure of the fayalite is finer than in any of the other slags and the glass content greater. The proportion of glass is similar to the proportion of the structure predicted to be iron cordierite from the ternary diagram, thus it seems likely that the iron cordierite is difficult to crystallize.

Discussion

The first question to be addressed is whether any of the slags could have been produced directly from the ores retrieved from the different sites. Mass balances were calculated in order to assess this. Examples of these for the B slags contained in Table 2 are given in Tables 4 and 5.

For the Balance 1, shown in Table 4, a number of assumptions were made. The first was that the contribution to the mass balance from the charcoal or wood ash can be ignored. The principal justification for this is that the yield of ash from wood or charcoal is typically of the order of 1%, and there is no consistent evidence in the present slags, except for those from Opi, of any significant contamination from ash of which a most likely oxide component is K_2O. Other oxides, particularly CaO, may come from the ash, but the ash composition is dependent on the soil conditions under which the tree grew and can thus be quite variable. The K_2O is higher in the Opi slags than any of the others as is demonstrated by the presence of leucite, and it is known that these slags have higher slag liquidus

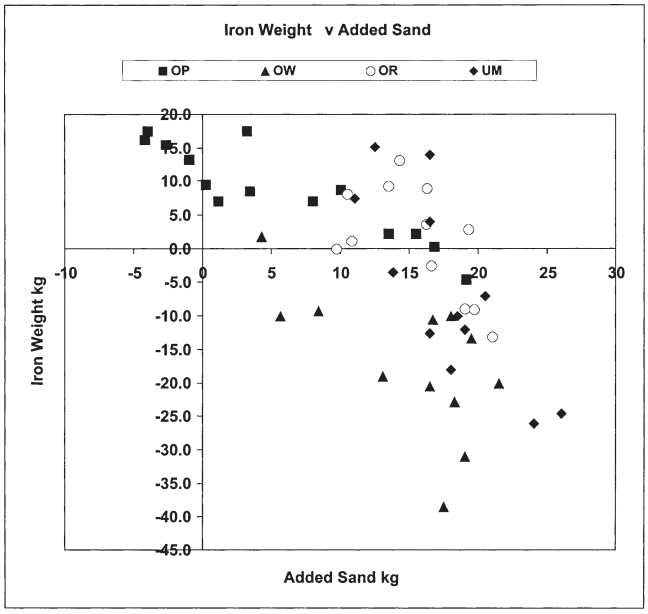

Figure 8: Influence of sand additions on the calculated iron weight.

temperatures that would require higher fuel consumption. The other reason for the assumption comes from work on bloomery furnaces by Tylecote *et al* (1971), which demonstrated that the low carbon content associated with most bloomery irons is also associated with free-running slags and a ratio of fuel used to metallic iron produced of less than 3:4. It is also likely that the contribution to the mass balance from the furnace structure is small, and the second assumption was that this can be ignored.

The balance shown in Table 4 was calculated on the basis of 100kg of ore, and assumes that all the alumina in the slag comes from the ore, hence on a weight basis the alumina contents of the slag and ore are equal. The amount of metallic iron produced is calculated on the assumption that the combined iron is in the form of Fe_2O_3 in the ore and FeO in the slag. The slag produced has the measured composition and the slag weight is calculated. In Table 4 the first four calculations use the mean ore composition of each site (from Table 3) and the slag composition of each 'B' sample (Table 2). Modest amounts of iron are obtained for the recent sites of Orba and Umundu with significant silica additions in each case. The Opi ore produces a considerable amount of iron but provides too much silica, so that silica has to be removed to make the balance, which is impracticable. The Owerre-Elu ore gives a negative iron production on this balance. The final calculation shows that the average ore composition cannot produce iron if the average analysis of the slags is to be obtained, an addition of silica would be required to make the balance.

To explore the effects of adding silica, a subsidiary balance was performed in which the average ore composition was used and the balance was forced to meet the alumina/silica ratio of each slag. The results of this are shown in Figure 8, which plots the weight of iron produced against the weight of added sand (assumed to be pure silica). It shows that a number of the slags found at Opi, Orba and Umundu could be made from ore of the average composition but with significant additions of silica. The requirement for a negative silica addition for the higher yield Opi slags confirms that the Opi ores were exceptionally rich in silica (Table 3) and that they could produce some of the analysed Opi slags without added sand. No Owerre-Elu slags could have been made from ores while producing useful amounts of iron, and the same is true for the majority of the Orba and Umundu slags. This suggests that either the current ores were not used to make the analysed slags or that some further ore

Table 5: Mass balance 2 for the 'B' slags of Table 2

Oxide	BALANCE 2					
	Ore (kg)	Sand (kg)	Iron in (kg)	Iron out (kg)	Slag (kg)	Slag (wt%)
OPB						
Fe_2O_3	82.9	0.0	58.0	39.2	24.2	61.1
Al_2O_3	7.0	0.0	0.0	-	7.0	17.7
SiO_2	7.1	0.0	0.0	-	7.1	17.8
Total	97.0	0.0	0.0	-	38.3	96.6
OWB						
Fe_2O_3	77.2	0.0	54.0	19.1	44.9	66.7
Al_2O_3	7.0	0.0	0.0	-	7.0	10.4
SiO_2	12.8	0.0	0.0	-	12.8	19.0
Total	97.0	0.0	0.0	-	64.7	96.1
ORB						
Fe_2O_3	72.2	0.0	50.6	30.0	26.4	49.8
Al_2O_3	7.0	0.0	0.0	-	7.0	13.2
SiO_2	17.8	0.0	0.0	-	17.8	33.5
Total	97.0	0.0	0.0	-	51.2	96.5
UMB						
Fe_2O_3	73.2	0.0	51.2	32.0	24.7	49.4
Al_2O_3	7.0	0.0	0.0	-	7.0	14.0
SiO_2	16.8	0.0	0.0	-	16.8	33.6
Total	97.0	0.0	0.0	-	48.5	97.0
Mean ore						
Fe_2O_3	73.4	0.0	51.7	23.3	36.4	58.8
Al_2O_3	7.0	0.0	0.0	-	7.0	11.3
SiO_2	16.2	0.0	0.0	-	16.2	26.1
Total	97.0	0.0	0.0	-	59.6	96.2

Note: Balance 2 calculates ore composition to give measured slag composition. For other assumptions see text.

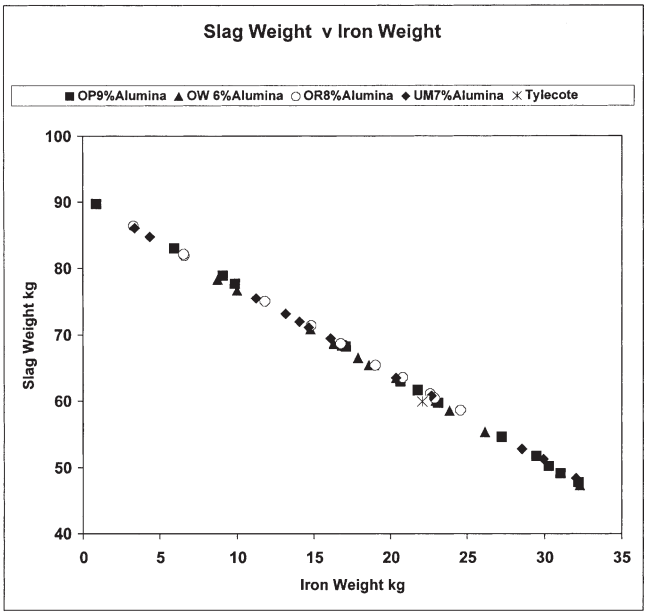

Figure 9: Slag and iron weights calculated from assumed 7% alumina contents of furnace charge.

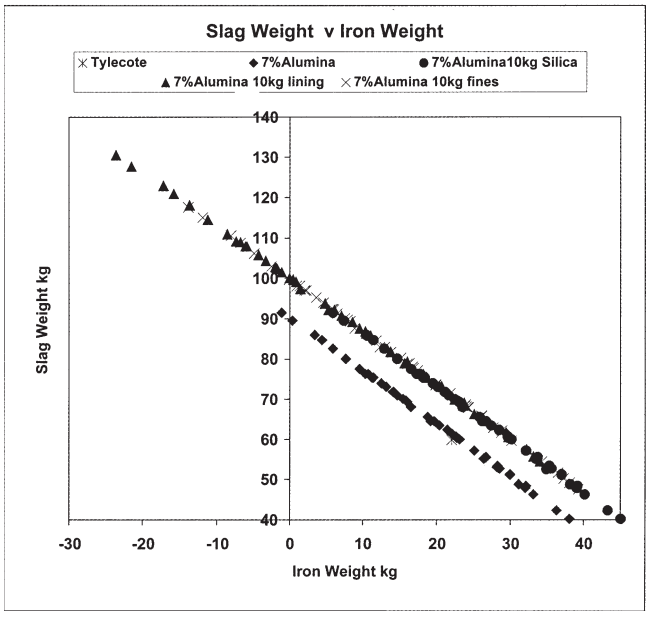

Figure 10: The calculated effect of adding of 10% each of sand, ore fines and furnace lining on slag and iron weight.

preparation had been used. Ethnographic information indicates that all the sites used sized ore, and Tylecote *et al* (1971) showed clearly that ore sizing is essential for efficient bloomery furnace operation in a shaft furnace with forced air draught. Morton and Wingrove (1974) suggested that for Carboniferous Period ores the sized ore provides a slag of appropriate composition, whereas for rich ores the ore fines provide the appropriate composition for the slag. The other observation from Morton and Wingrove (1972) is that the slag and ore have approximately the same ratio of alumina-to-silica, a feature found also by Todd (1984) for Ethiopian slags, but which was not the case in the present work.

To get another view on the relationship between ore, slag and iron yield, mass Balance 2, shown in Table 5, was calculated. This reverses the calculation to find the ore composition required to give the measured slag analysis on the basis of an assumed ore alumina content of 7%. The other assumption is that the sum of the Fe_2O_3, SiO_2 and Al_2O_3 contents of the ore totalled 97%, which was true for most of the ores analysed. No additions of silica were made. This results in outputs of iron ranging from 19 to 39kg for each 100kg of ore, and iron is made at all the sites using the 'B' slag compositions. Similar balance calculations were performed for all the analysed slags at alumina levels from 6% to 10%. Figure 9 shows the slag and corresponding iron weights predicted from these calculations. It shows the alumina level in the ores needed to produce iron for all the analysed slags from the particular site. An ore with 9% alumina is required at Opi, 8% at Orba, 7% at Umundu and 6% at Owerre-Elu. The result of an experimental melt by Tylecote *et al* (1971) is also shown, and this point lies close to the calculated line. These calculations assume that no silica is added, yet the ethnographic evidence suggests that some sand was added to the furnace at Orba. It is possible that this could have been ore fines, but it seems likely that fines would have had a higher level of silica and alumina than the sized ore (Morton and Wingrove 1974).

To probe further into the consequences of making accidental or intended additions, the effects of adding silica, ore fines and furnace lining to the slag was also

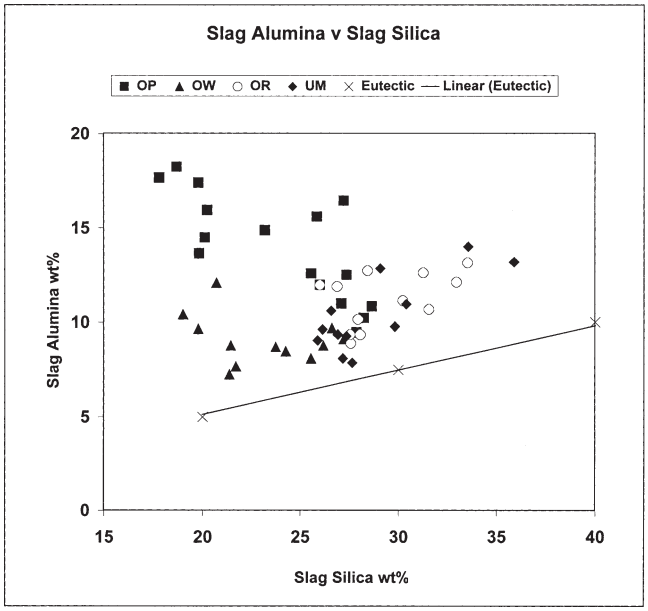

Figure 11: Relationship between measured alumina and silica contents of the slags.

tested in similar balances. Figure 10 shows the effect of additions of 10kg of silica, 10kg of furnace lining and 10kg of ore fines on the output of iron and the slag volume for an original ore with 7% alumina. Adding sand (silica) increases the slag volume by 10kg but also increases the iron output as the silica replaces that which would have come from the ore. The furnace lining was assumed to be essentially a clay mineral with a composition of 50% SiO_2, 30% Al_2O_3 and 20% Fe_2O_3, this addition also increases the slag volume by 10kg for any iron level, but reduces the iron output for any given slag composition by more than 20kg. This effect is largely due to the increase in alumina. Any loss of furnace lining to the slag is therefore very deleterious. The ore fines were assumed to be 50% Fe_2O_3, 20% Al_2O_3 and 30 % SiO_2. Again the slag volume is increased and the iron output decreased. The decrease in iron is again due to the increase in alumina. Although the assumed compositions used in the calculations are rather arbitrary, the effect of alumina on decreasing the iron output is very clear and it might now be possible to infer whether additions of sand, fines and lining have influenced the compositions of the analysed slags. It is possible that small additions of sand were made in most of the smelting operations that produced the slags. Alternatively small additions of ore fines might have been made, which would probably have assisted in forming an initial liquid phase and helped to flux the sized lump ore.

Figure 11 shows the relationship between the measured alumina and silica contents of the slags. The Opi slags appear as two clear groups (Fig 2b): those with silica below 21% and those with alumina below 13%, with three slags of intermediate contents. The low-silica slags can be made from an ore similar to the mean ore composition with fluctuations in SiO_2. The slag silica shows a greater standard deviation of 3.8% for the Opi site compared with about 2.5% for the other three sites. It is likely that these slags represent the first attempts to make iron at this ancient site, and resulting iron outputs would have been between 10 and 20kg. The lower alumina slags could be made from the mean ore composition with silica additions of between about 15 and 20kg. If this were done, the iron yield would have been considerably lower, typically about 2kg. The three intermediate slags require smaller silica additions and would have produced intermediate quantities of iron. It seems most unlikely that additions would have been made that reduce the output of iron, particularly as a larger output of iron can be obtained if the ore alumina is lowered (see Table 5). This might have been achieved by sizing the ore and using only particular fractions,

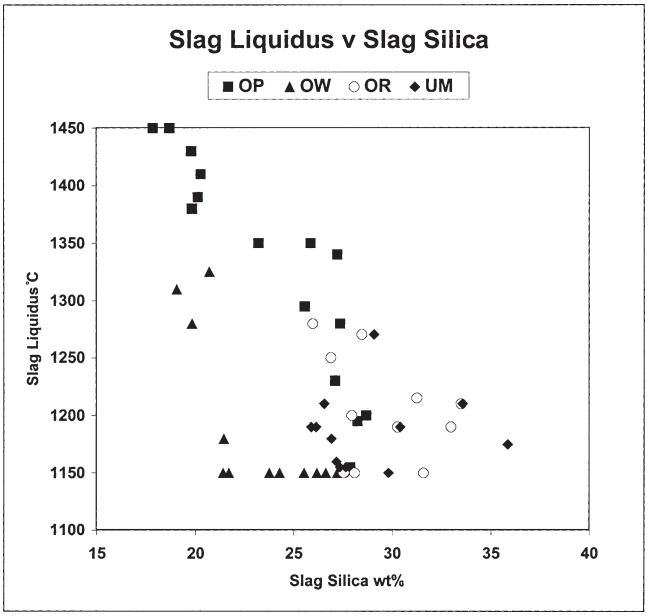

Figure 12: Estimated slag liquidus temperatures (from Figure 2) as a function of measured slag silica (wt%).

support for which is provided by ethnographical evidence that sized ore was used at each site. If sizing had taken place at Opi it is likely that it would have been continued at all the later sites.

The slags from Owerre-Elu, the second oldest site, also divide into two groups in Figure 11, with a group below about 22% silica and a group with higher silica levels. It is only possible to produce iron from the average ore analysis with an addition of 4kg of silica, giving the slag with the highest alumina content, but the iron output is only 2kg. All the other Owerre-Elu slags must have been made from ore with a lower alumina content, which also might have been obtained by ore sizing. Another benefit of using ores with lower alumina is clearly seen as the values of slag silica and alumina approach the line associated with the eutectic valleys in the ternary diagram, which is shown as a line in Figure 11. The Owerre-Elu slags require an alumina level lower than any other site. It seems likely that the ore selection required to control the alumina level was well developed. It is possible that the ores were crushed to change the alumina and silica levels, but no evidence of ore roasting has been discovered at any of the sites.

The other effect of using a lower alumina ore at both these early sites is that the slag liquidus inferred from the ternary diagram in Figure 2 is lowered, and the slags are thus likely to be both more workable and the microstructures rather finer. Figure 12 shows the variation of slag liquidus with measured slag silica, for all the analysed slags. It is notable that the slags from

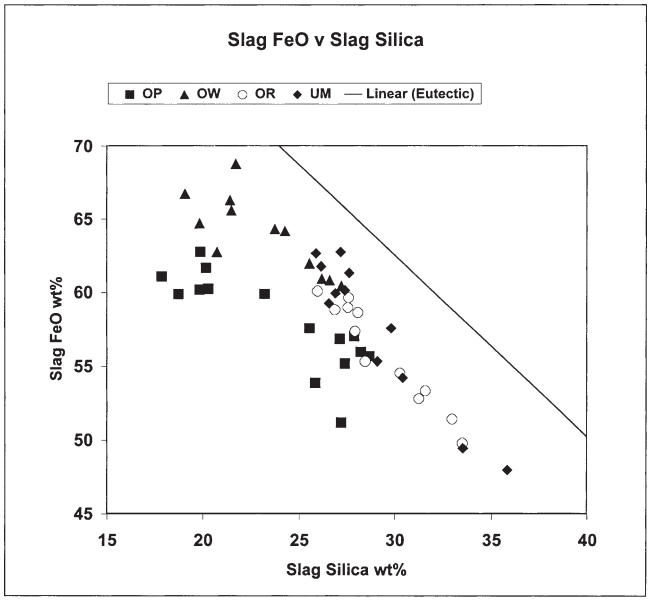

Figure 13: Variation of measured slag FeO versus silica for all the slags analysed.

the later sites approach the lower limit of slag liquidus provided by the eutectic valleys in the ternary diagram. Although Opi slags tend to have liquidus significantly higher than the eutectic values, the other early site of Owerre-Elu has nearly all its slags very close to the lower limit. This suggests that the ore sizing might have been done to give a lower temperature liquidus.

A plot of slag FeO against slag silica is shown in Figure 13. Most of the slags with low FeO are associated with the modern sites at Umundu and Owerre-Elu. The question is: does this reflect a change in furnace type or a change in furnace practice? It is interesting to note that Tylecote *et al* (1971) claim that, in order to have a tappable slag, the FeO content must be greater than 46%. The lowest quantity of FeO in the present slags was 47%. Slags with less FeO than this would be in another constitutive triangle in which primary hercynite is replaced by primary tridymite.

The two most recent sites at Orba and Umundu have rather similar characteristics in that they operated on an induced draught and the slag was raked out as an agglomerate. This operation requires a more fluid slag, and the microstructure of the slag, which is very fine, suggests a rapid cooling rate compared with the slags tapped at the earlier sites. The slag FeO content of 47% is approaching the limit that is free-running. The calculated iron yield from these two sites is greater than that obtained at the earlier sites due to the decrease in slag FeO and the reduction in slag volume. Because of the higher alumina content, the slag liquidus is not as low as the lowest-melting Owerre-Elu slags, and this shows that slag liquidus is only one of the factors influencing slag fluidity. The calculated alumina and silica proportions in the initial ore are very much further from that found in the available ores. The report of sand additions at Orba could well be true but it is also possible that this "sand" is ore fines which might contain higher levels of silica and alumina than the lump ore. Both additions would result in an increase in slag volume, and, if the fines had a high alumina content, the iron yield would be much reduced. It would seem that additions of silica are more likely.

The sand additions in the Nsukka slags were not black sand as been reported in Modakeke, south-west Nigeria, by Inge and Rehren(2003), as the titania content of the slags was very similar to that of the ores at about 1 to1.5% TiO_2. The Modakeke slags contained between 6.6 and 11.1% TiO_2.

Conclusions

From carbon dating of charcoal associated with the slags and ethnographic evidence of recent working, it is known that there has been bloomery iron making in the Nsukka region of Nigeria for over two millennia up to the recent past. The composition and microstructure of slags and ores from four sites have been quantitatively analysed in the SEM. The slag components are predominantly FeO, Al_2O_3 and SiO_2 and can be represented on the ternary diagram for this system. The phases present are broadly predictable from this phase diagram, but with some significant differences.

The earliest site, Opi, has some slags of a composition that could be directly smelted from existing ores, but only with very high slag liquidus temperatures. Other slags from the site would require ores richer in silica than those found currently. Only a few of the other slags from Orba and Umundu could be made from existing ores to produce a good yield of iron. Due to the changes in slag composition found at Opi and Owerre-Elu it seems likely that some ore preparation was undertaken; certainly the ore was sized.

Most of the modern slags contained the three microstructural phases fayalite, hercynite and glass. The iron making at these sites (Umundu and Orba) was considerably more efficient with greater iron yield and lower slag volumes, and the microstructures of the agglomerated raked slag were very fine due to their rapid cooling. The slag liquidus approached the minimum possible in the ternary system but the elevated

levels of alumina in most slags prevented this minimum being achieved.

It is possible that the addition of sand reported at Orba was used to provide the higher silica levels found in the slags. Alternatively the sand might have been ore fines which would produce a large reduction in iron output, due to their high alumina levels, but might flux the lump ore. It seems more likely that sand was added. The addition of sand would have produced an increase in slag bulk, but would also have increased the iron output and lowered the slag liquidus temperature.

Acknowledgements

Our thanks are due to the British Council for supporting E E Okafor during this work. Thanks are also due to Dr S Murphy for much useful discussion.

References

Allen J R L 1988, 'Chemical composition patterns in Romano-British bloomery slags from the wetlands of the Severn estuary' *Historical Metallurgy* 22 (2), 81–6.

Bachmann H-G 1982, 'The identification of slags from archeological sites', *London Institute of Archeology Occasional Publication 6*, 1–20.

Benevuti N, Mascaro I, Costagliola P, Tanelli G and Romualdi A 2000 'Iron, copper and tin at Baratti (Populonia): smelting processes and metal provenances', *Historical Metallurgy* 34(2), 67–76.

Challis K 2002, 'A medieval iron smelting site at Stanley Grange, Derbyshire', *Historical Metallurgy* 34(1), 33–42.

Durman M and Murphy S 1994, 'The creep behaviour of zinc-aluminium based alloys with 0% to 30% Al' in G Torres-Villaseñor, Y H Zhu and C Piña-Barba (eds), *Advances in science, technology and applications of Zn-Al alloys* (Mexico City), 59–67.

Goucher C L 1981, 'Iron is iron till it rusts: trade and ecology in the decline of West African iron smelting', *Nyame Akuma* 23, 36.

Høst-Madsen L and Buchwald V F 1999, 'The characterization and provenancing of ore, slag and iron from the Iron Age settlement at Snorup', *Historical Metallurgy* 33(2), 57–67.

Inge A and Rehren T 2003, 'Black sand and ironstone: iron smelting in Modakeke, Ife, south western Nigeria', *Institute for Archeo-Metallurgical Studies News* No. 23, 15–20.

Keissling R and Lange N 1964, *Non-metallic inclusions in steel Publ no. 76* (London).

Lewin E M, Robbins C R and McMurdie H F 1964, *Phase diagrams for ceramists* (Ohio).

Morton G R and Wingrove J 1969, 'Constitution of bloomery slags; Part 1: Roman', *JISI* 207, 1556–69.

Morton G R and Wingrove J 1972, 'Constitution of bloomery slags; Part 2: Medieval', *JISI* 210, 478–88.

Okafor E E 1992, Early iron smelting in Nsukka, Nigeria: information from slags and residues PhD thesis, University of Sheffield.

Photos-Jones E, Atkinson J A, Hall A J and Banks I 1998, 'The bloomery mounds of the Scottish highlands. Part 1: the archaeological background', *Historical Metallurgy* 32(1), 15–32.

Stuiver M and Pearson G W 1986, 'High-precision calibration of the radiocarbon time scale, AD 1950–500 BC', *Radiocarbon* 28, 805–38.

Todd J A 1979, 'Studies of the African iron age', *Journal of Metals* 31(11), 39–45

Todd J A 1984, 'The relationship between ore, slag and metal composition in pre-industrial iron', in Ronig A D and Goldstein J A (eds), *Microbeam Analysis* (San Francisco), 235–8.

Todd J A and Charles J A 1978, 'Ethiopian bloomery iron and the significance of inclusion analysis in iron studies', *Historical Metallurgy* 12(2), 63–87.

Tylecote R F 1975, 'The origin of iron smelting in Africa' *West African Journal of Archeology* 5, 1–9.

Tylecote R F, Austin J N and Wraith E A 1971, 'The mechanism of the bloomery process in shaft furnaces', *JISI* 209, 342–63.

van der Meerwe N J 1980, 'The advent of iron in Africa', in Wertime T A and Mulphy D J (eds), *The Coming of Age of Iron* (London), 463–506.

van der Plicht J and Mook W G 1989, 'Calibration of radio carbon by computer', *Radiocarbon* 31, 805–816.

The authors

John A Whiteman is a metallographer interested in the application of SEM and TEM analysis to materials technology problems. He has recently retired from his post as Senior Lecturer in the Department of Engineering Materials at the University of Sheffield.
Address: Department of Engineering Materials, The University of Sheffield, St George's Square, Sheffield S1 3JD, UK.
e-mail: j.whiteman@sheffield.ac.uk

Edwin E Okafor is a field archaeologist concerned with understanding the development of iron smelting in the Nok culture. He is currently Professor and Head of Department of Archeology at the University of Nigeria.
Address: Department of Archeology, University of Nigeria, Nsukka, Nigeria.